Supplementary Information

Application of Solid-State NMR Restraint Potentials in Membrane Protein Modeling

Jinhyuk Lee[a], Jianhan Chen[b], Charles L. Brooks III[c], and Wonpil Im[a,*]

[a] Department of Molecular Biosciences and Center for Bioinformatics
The University of Kansas, 2030 Becker Drive, Lawrence, KS 66047
[b] Department of Biochemistry, The Kansas State University,
141 Chalmers Hall, Manhattan, KS 66506
[c] Department of Chemistry, The University of Michigan,
930 North University Avenue, Ann Arbor, MI 48109

Keywords: molecular dynamics, transmembrane helices, orientation restraint, ^{15}N chemical shift, ^{15}N-^{1}H dipolar coupling

S.1 The derivatives of dipolar coupling restraint potential

The angle θ in Eq. (1) is the angle between the N-H internuclear vector, $\mathbf{r}_{\mathrm{NH}}$, and the magnetic field, $\hat{n} \equiv \hat{z}$,

$$\cos\theta = \frac{\mathbf{r}_{\mathrm{NH}} \cdot \hat{n}}{|\mathbf{r}_{\mathrm{NH}}|} = \frac{z_{\mathrm{NH}}}{|\mathbf{r}_{\mathrm{NH}}|}, \tag{S1}$$

where z_{NH} is the z component of $\mathbf{r}_{\mathrm{NH}}$. The derivative of $\cos\theta$ with respect to $\mathbf{r}_\alpha$ ($\alpha =$ N or H) becomes

$$\frac{\partial \cos\theta}{\partial \mathbf{r}_\alpha} = \frac{1}{|\mathbf{r}_{\mathrm{NH}}|}\frac{\partial z_{\mathrm{NH}}}{\partial \mathbf{r}_\alpha} - \frac{z_{\mathrm{NH}}}{|\mathbf{r}_{\mathrm{NH}}|^2}\frac{\partial |\mathbf{r}_{\mathrm{NH}}|}{\partial \mathbf{r}_\alpha}\ , \tag{S2}$$

where the derivative of $|\mathbf{r}_{\mathrm{NH}}|$ is

$$\frac{\partial |\mathbf{r}_{\mathrm{NH}}|}{\partial \mathbf{r}_\alpha} = \frac{1}{|\mathbf{r}_{\mathrm{NH}}|}\left(x_{\mathrm{NH}}\frac{\partial x_{\mathrm{NH}}}{\partial \mathbf{r}_\alpha} + y_{\mathrm{NH}}\frac{\partial y_{\mathrm{NH}}}{\partial \mathbf{r}_\alpha} + z_{\mathrm{NH}}\frac{\partial z_{\mathrm{NH}}}{\partial \mathbf{r}_\alpha}\right). \tag{S3}$$

The derivatives of η_{NH} ($\eta = x$, y, or z) with respect to the N atom coordinate ζ_{N} ($\zeta = x$, y, or z) becomes

$$\frac{\partial \eta_{\mathrm{NH}}}{\partial \zeta_{\mathrm{N}}} = \begin{cases} -1 & \eta = \zeta \\ 0 & \eta \neq \zeta. \end{cases} \tag{S4}$$

Similarly, the derivatives of η_{NH} with respect to the H atom coordinate ζ_{H} becomes

$$\frac{\partial \eta_{\mathrm{NH}}}{\partial \zeta_{\mathrm{H}}} = \begin{cases} 1 & \eta = \zeta \\ 0 & \eta \neq \zeta. \end{cases} \tag{S5}$$

In the case that the NH distance varies during a simulations, the derivative of the dipolar coupling constant, $\nu_0 = (\gamma_N \gamma_H h \mu_0)/(8\pi^3 |\mathbf{r}_{\mathrm{NH}}|^3)$, becomes

$$\frac{\partial \nu_0}{\partial \mathbf{r}_\alpha} = \frac{-3\nu_0}{|\mathbf{r}_{\mathrm{NH}}|}\frac{\partial |\mathbf{r}_{\mathrm{NH}}|}{\partial \mathbf{r}_\alpha}. \tag{S6}$$

Utilizing these equations, one can obtain the full expression of the derivatives of the dipolar coupling in Eq. (4).

S.2 The derivatives of chemical shift restraint potential

In Eq. (10), the derivatives of the z components ($\hat{e}_{i,z}$) of the unit chemical shift tensors, $\hat{e}_i$ ($i = 1, 2, 3$), with respect to $\mathbf{r}_\alpha$ become

$$\frac{\partial \hat{e}_{i,z}}{\partial \mathbf{r}_\alpha} = \frac{\partial}{\partial \mathbf{r}_\alpha}\left(\frac{e_{i,z}}{|\mathbf{e}_i|}\right) = \frac{1}{|\mathbf{e}_i|}\frac{\partial e_{i,z}}{\partial \mathbf{r}_\alpha} - \frac{e_{i,z}}{|\mathbf{e}_i|^2}\frac{\partial |\mathbf{e}_i|}{\partial \mathbf{r}_\alpha} \ , \tag{S7}$$

where $\mathbf{e}_i = |\mathbf{e}_i|\,\hat{e}_i$ and $e_{i,z}$ is the z component of $\mathbf{e}_i$. The derivative of the magnitude of the chemical shift tensor vectors, $\mathbf{e}_i$, becomes

$$\frac{\partial |\mathbf{e}_i|}{\partial \mathbf{r}_\alpha} = \frac{1}{|\mathbf{e}_i|}\left(e_{i,x}\frac{\partial e_{i,x}}{\partial \mathbf{r}_\alpha} + e_{i,y}\frac{\partial e_{i,y}}{\partial \mathbf{r}_\alpha} + e_{i,z}\frac{\partial e_{i,z}}{\partial \mathbf{r}_\alpha}\right) \ . \tag{S8}$$

As mentioned in the main text, $\mathbf{e}_1$, $\mathbf{e}_2$, and $\mathbf{e}_3$ are defined in terms of the peptide plane made by N, C, and H atoms. In general, $\mathbf{e}_1$ and $\mathbf{e}_3$ are on the peptide plane, and $\mathbf{e}_2$ is defined by the cross product of $\mathbf{r}_{\rm NC}$ and $\mathbf{r}_{\rm NH}$. Then, $\mathbf{e}_1$ is defined by a rotation angle ϕ from $\mathbf{r}_{\rm NH}$ on the peptide plane, and $\mathbf{e}_3 = \mathbf{e}_1 \times \mathbf{e}_2$. Alternately, by introducing $\mathbf{r}_p = \mathbf{r}_{\rm NH} \times \mathbf{e}_2$ and $\delta = \phi$ - 90°, a angle between $\mathbf{e}_3$ and $\mathbf{r}_{\rm NH}$, one can simplify the expressions of $\mathbf{e}_i$ as follows;

$$\mathbf{e}_1 = (x_{\rm NH}\,\cos\phi + x_{\rm p}\,\sin\phi)\hat{x} + (y_{\rm NH}\,\cos\phi + y_{\rm p}\,\sin\phi)\hat{y} + (z_{\rm NH}\,\cos\phi + z_{\rm p}\,\sin\phi)\hat{z} \tag{S9}$$

$$\mathbf{e}_2 = (y_{\rm NH}\,z_{\rm NC} - z_{\rm NH}\,y_{\rm NC})\hat{x} + (z_{\rm NH}\,x_{\rm NC} - x_{\rm NH}\,z_{\rm NC})\hat{y} + (x_{\rm NH}\,y_{\rm NC} - y_{\rm NH}\,x_{\rm NC})\hat{z} \tag{S10}$$

$$\mathbf{e}_3 = (x_{\rm NH}\,\cos\delta + x_{\rm p}\,\sin\delta)\hat{x} + (y_{\rm NH}\,\cos\delta + y_{\rm p}\,\sin\delta)\hat{y} + (z_{\rm NH}\,\cos\delta + z_{\rm p}\,\sin\delta)\hat{z} \ , \tag{S11}$$

where

$$\mathbf{r}_p = (y_{\rm NH}\,e_{2,z} - z_{\rm NH}\,e_{2,y})\hat{x} + (z_{\rm NH}\,e_{2,x} - x_{\rm NH}\,e_{2,z})\hat{y} + (x_{\rm NH}\,e_{2,y} - y_{\rm NH}\,e_{2,x})\hat{z} \tag{S12}$$

It becomes clear that solving Eq. (S7) involves the derivatives of $\eta_{\rm NH}$, $\eta_{\rm NC}$, and $\eta_{\rm p}$ ($\eta = x, y, z$) with respect to $\mathbf{r}_\alpha$ ($\alpha =$ N, H, and C atoms). Equations (S4) and (S5) describes the derivatives of $\eta_{\rm NH}$ with respect to $\mathbf{r}_{\rm N}$ and $\mathbf{r}_{\rm H}$. Similarly, one can obtain the derivatives of $\eta_{\rm NC}$ with respect to $\mathbf{r}_{\rm N}$ and $\mathbf{r}_{\rm C}$;

$$\frac{\partial \eta_{\rm NC}}{\partial \zeta_{\rm N}} = \begin{cases} -1 & \eta = \zeta \\ 0 & \eta \neq \zeta \end{cases} \tag{S13}$$

$$\frac{\partial \eta_{\mathrm{NC}}}{\partial \zeta_{\mathrm{C}}} = \begin{cases} 1 & \eta = \zeta \\ 0 & \eta \neq \zeta \end{cases} \tag{S14}$$

Therefore, Eq. (S7) can be analytically solved using Eqs. (S8) and (S9)-(S11) through Eqs. (S4), (S5), (S13), and (S14).

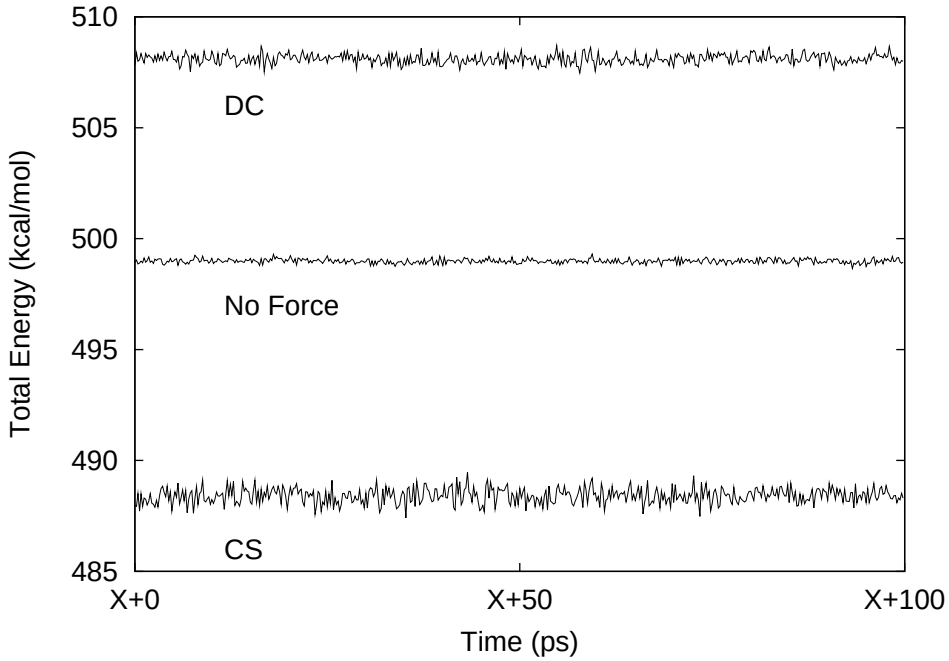

Figure S1. Total energy profiles as a function of time during 100 ps NVE Cartesian MD simulations without the SSNMR restraint potentials, with the chemical shift restraint potential (CS) with $k_{\mathrm{cs}} = 0.05$ kcal/(mol·ppm^2), and with the dipolar coupling restraint potential (DC) with $k_{\mathrm{dc}} = 1.0$ kcal/(mol·kHz^2).

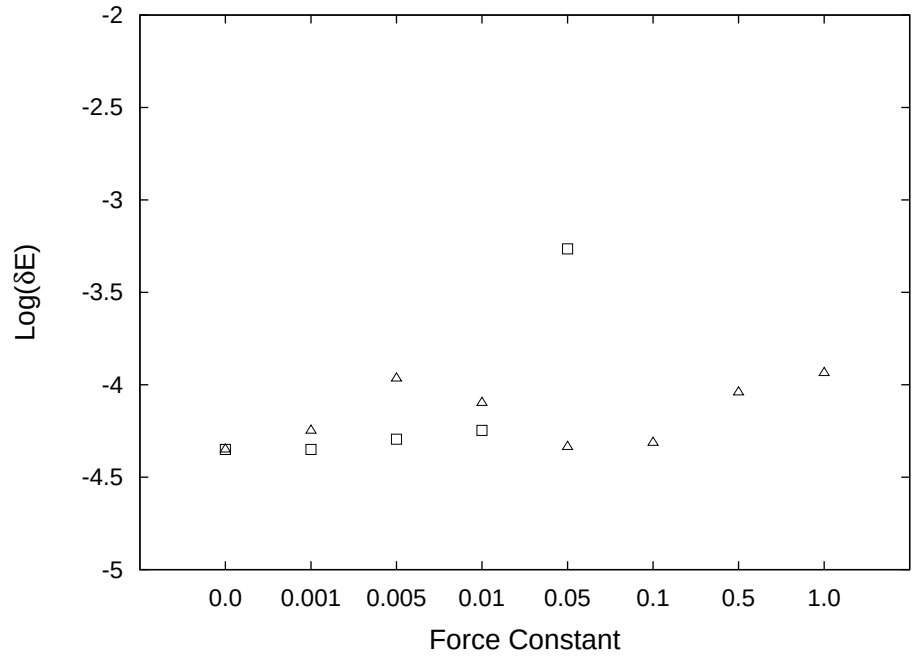

Figure S2. Total energy fluctuations (δE) of 100 ps NVE Cartesian MD simulations as a function of k_{cs} (kcal/(mol·ppm^2), $\square$) and k_{dc} (kcal/(mol·kHz^2, $\triangle$): $\delta \mathrm{E} = (\langle \mathrm{E}^2 \rangle - \langle \mathrm{E} \rangle^2) / \langle \mathrm{E}_k \rangle)$, where E and E_k are the total energy and the kinetic energy, respectively.

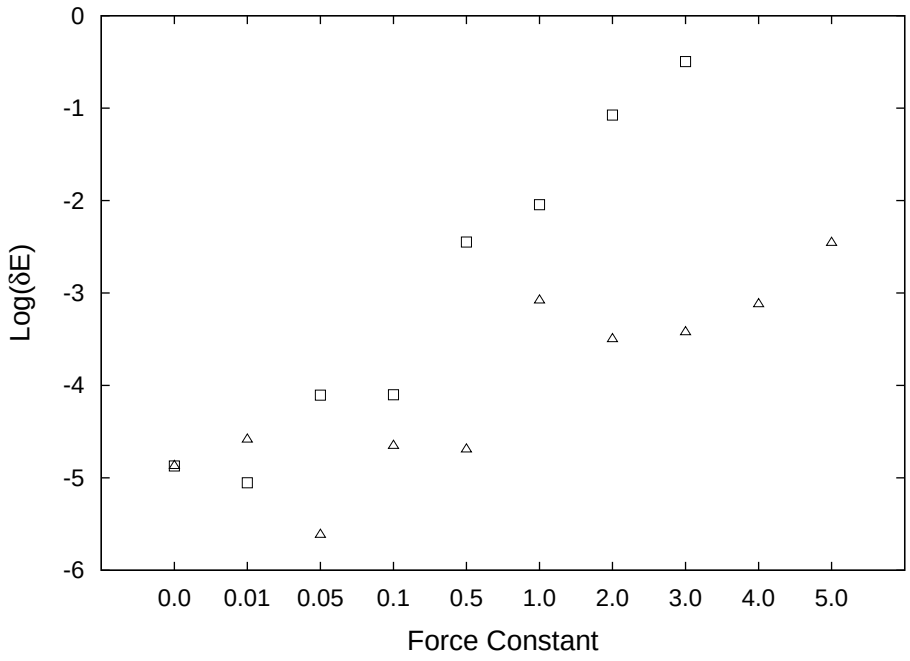

Figure S3. Total energy fluctuations (δE) of 100 ps NVE TAMD simulations as a function of k_{cs} ($\square$) and k_{dc} ($\triangle$). The definition of δE as well as the units of k_{cs} and k_{dc} are given in Fig. S2.

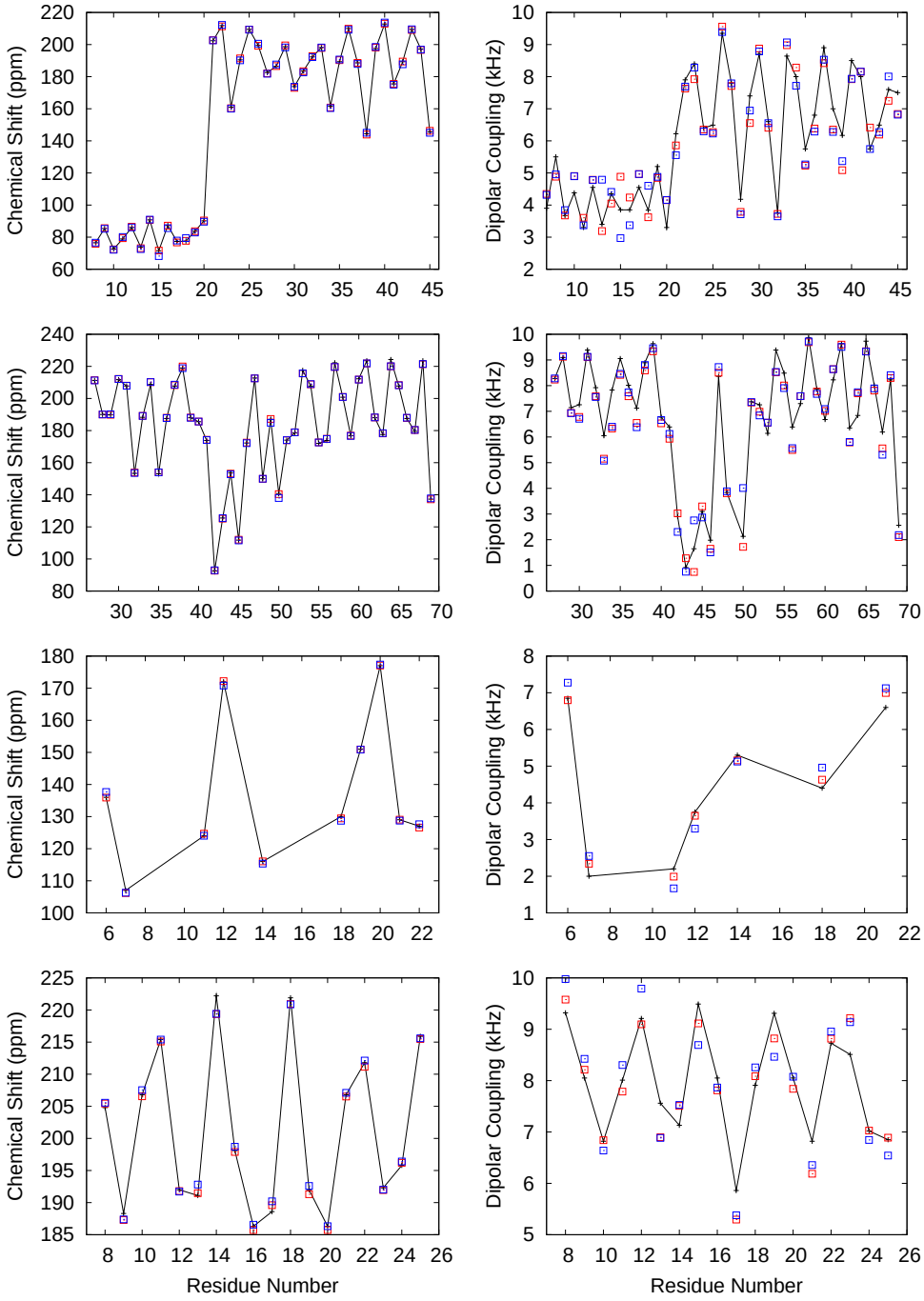

Figure S4. The experimental (solid line with + symbols) observables and the calculated values for the best (red) and worst (blue squares) structures in terms of RMSD of SSNMR observables ($\delta\sigma$ and $\delta\nu$) in vacuum (from top to bottom: fd coat, MerF, M2TMP, and VpuTM). The best/worst $\delta\sigma$ and $\delta\nu$ are 0.49/0.98 ppm and 0.95/0.99 kHz (fd coat), 1.05/1.16 ppm and 1.00/1.19 kHz (MerF), 0.41/0.86 ppm and 0.48/0.95 kHz (M2TMP), and 0.81/0.98 ppm and 0.88/0.99 kHz (VpuTM).

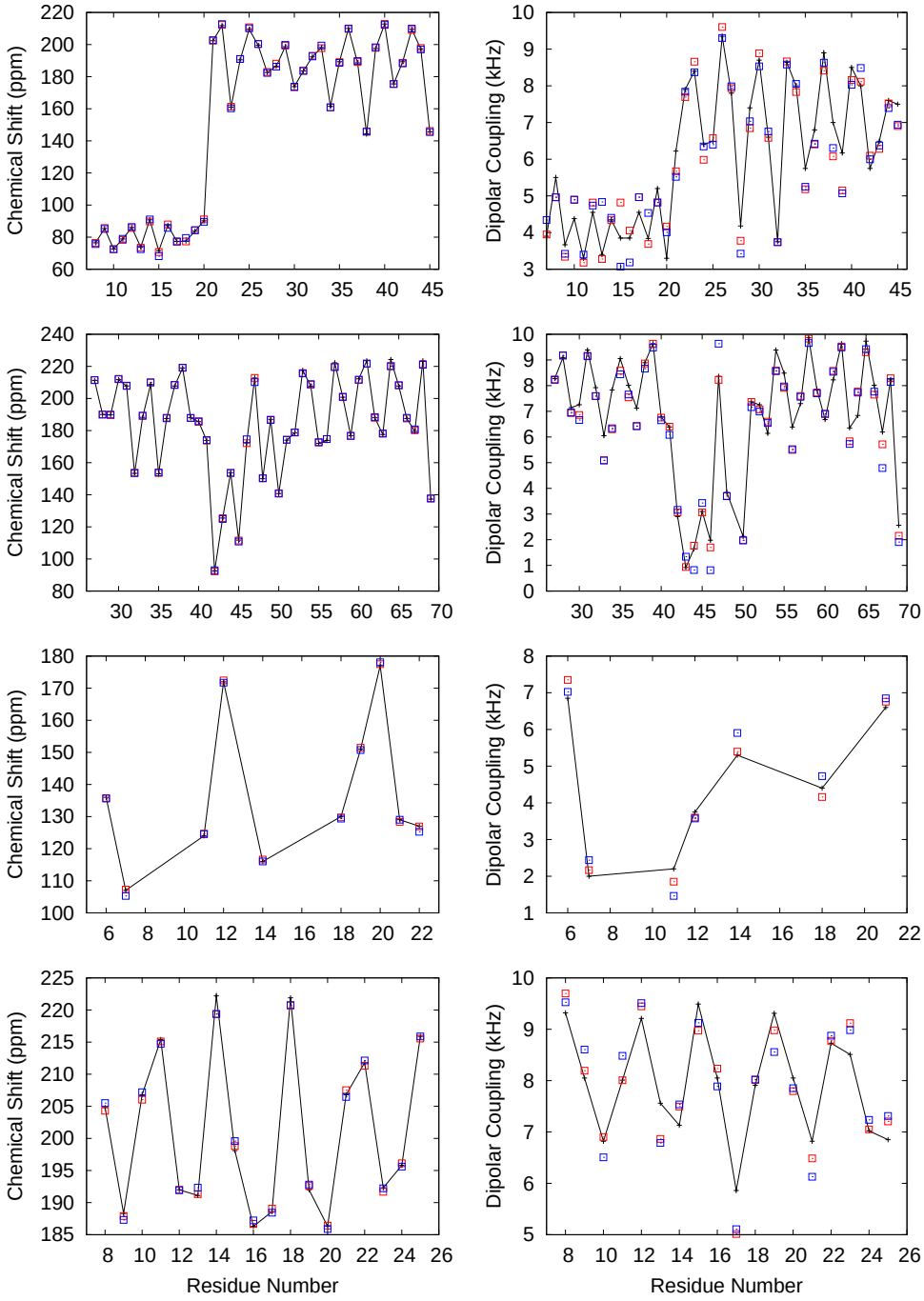

Figure S5. The experimental (solid line with + symbols) observables and the calculated values for the best (red) and worst (blue squares) structures in terms of RMSD of SSNMR observables ($\delta\sigma$ and $\delta\nu$) in GBSW (from top to bottom: fd coat, MerF, M2TMP, and VpuTM). The best/worst RMSDs of $\delta\sigma$ (left) and $\delta\nu$ (right) are 0.64/0.86 ppm and 0.93/0.99 kHz (fd coat), 0.98/1.20 ppm and 0.92/1.20 kHz (MerF), 0.45/0.90 ppm and 0.54/0.87 kHz (M2TMP), and 0.86/0.97 ppm and 0.77/0.93 kHz (VpuTM).

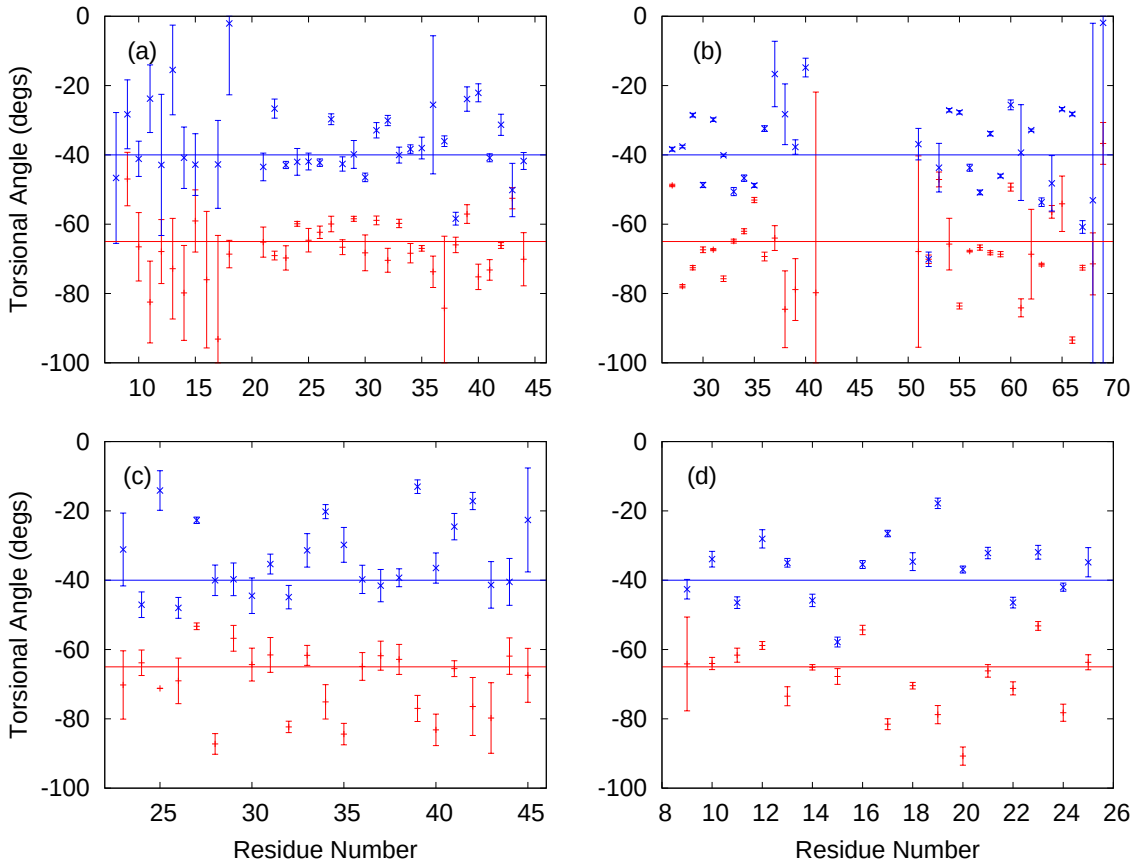

Figure S6. The torsion angles, ϕ (red) and ψ (blue), distributions of four monomers (a: fd coat, b: MerF, c: M2TMP, and d: VpuTM) in vacuum. The values are averaged over the structures satisfying the selection criteria. The lines at -65° and -40° represent the torsion angles ϕ (red) and ψ (blue) of ideal α-helix. The connecting loop regions (fd coat: residues 19-20 and MerF: residues 42-50) are removed for clarity.

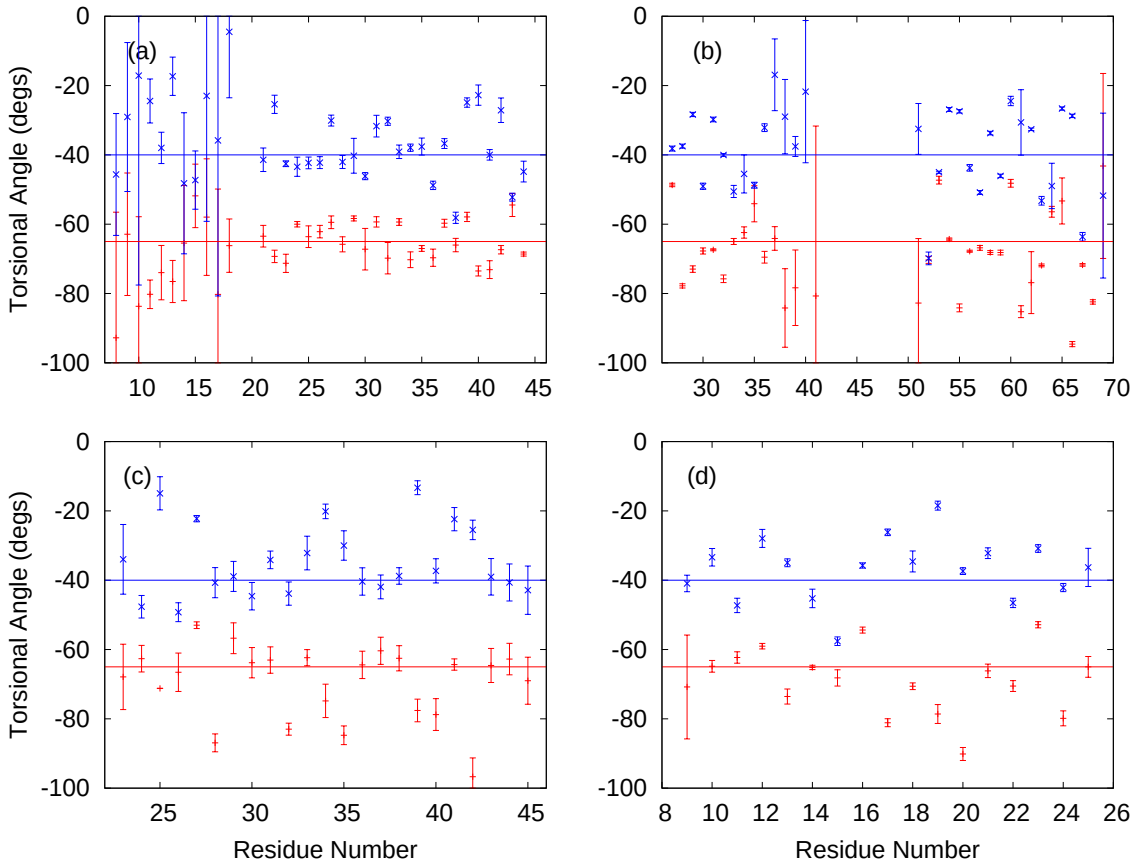

Figure S7. The torsion angles, ϕ (red) and ψ (blue), distributions of four monomers (a: fd coat, b: MerF, c: M2TMP, and d: VpuTM) in GBSW. The values are averaged over the structures satisfying the selection criteria. The lines at -65° and -40° represent the torsion angles ϕ (red) and ψ (blue) of ideal α-helix. The connecting loop regions (fd coat: residues 19-20 and MerF: residues 42-50) are removed for clarity.

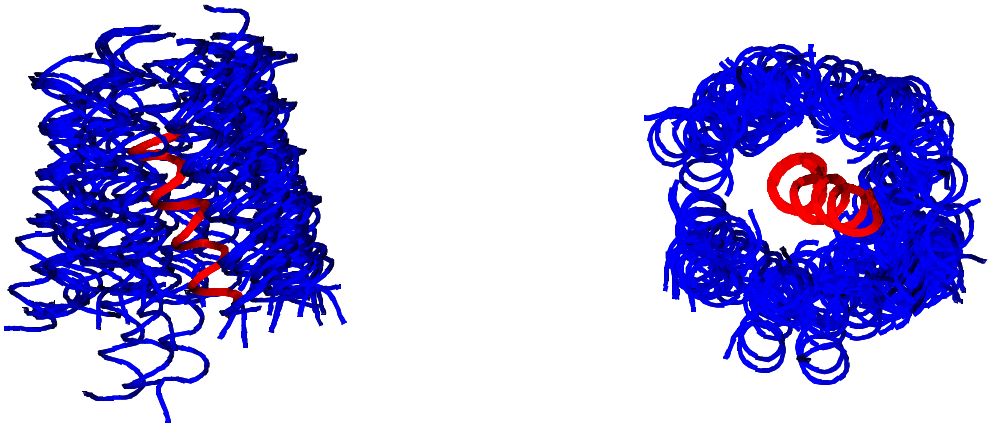

Figure S8. TM1-TM2 orientations of determined MerF structures: (left) a side view and (right) the bottom view. The TM1 domains (red) of individual MerF structures are superimposed to show the relative orientations of the TM2 domains (red). The connecting loop regions are removed for clarity.